

P300 spatial filtering and Coherence-based Channel selection

Gabriel Pires

Institute for Systems and Robotics
University of Coimbra
3000 Coimbra, Portugal
Email: gpires@isr.uc.pt

Urbano Nunes

Institute for Systems and Robotics
University of Coimbra
3000 Coimbra, Portugal
Email: urbano@isr.uc.pt

Miguel Castelo-Branco

Biomedical Inst. for Research in Light and Image
University of Coimbra
3000 Coimbra, Portugal
Email: mcbranco@ibili.uc.pt

Abstract—Spatial filtering is an important technique used in electroencephalography to enhance signal-to-noise ratio and to reduce the data dimensionality. In the context of Brain-Computer Interfaces, the Common Spatial Patterns method is widely used for classification of motor imagery events, however it is not very often used for classification of event related potentials such as P300. In this paper we show that Common Spatial Patterns is an effective approach to improve P300 classification rates. It is proposed a Bayesian methodology for feature combination that overcomes the limitations of the feature method used in motor imagery. Also, a method for channel selection based on inter-channel coherence is proposed, reducing the number of channels and improving the classification results.

I. INTRODUCTION

Brain computer Interface (BCI) based on P300 event related potential (ERP) proved to be an effective communication channel for people affected by severe motor disabilities. The first P300-based BCI was proposed by Farwell and Donchin [1] and since then, their seminar work as been followed by many other researchers. EEG signals are characterized by a very poor spatial resolution and the signal of interest has a very low signal-to-noise ratio. Working toward an effective BCI motivates the researchers to investigate methods that can increase communication bandwidth (ideally with single-trial) and reduce the channel dimension. To reach these goals, spatial filtering plays an important role and is an indispensable processing step for the feature extraction and pattern classification. Spatial filters can accentuate the signal of interest and at the same time attenuate the ongoing EEG and the non-EEG artifacts. In [2], the authors compare reference filter methods such as Common Average Reference, Small Laplacian and Large Laplacian with conventional ear reference, and show the improvement obtained with these spatial filters. They act as high-pass spatial filters that enhance local activity and decrease the distributed activity.

A different approach named Common Spatial Patterns (CSP) was proposed by Koles [3]. It was applied in clinical electroencephalography for localization of sources of specific neurophysiologic components and to extract high frequency spike and sharp wave components from the EEG of neurologic patients. The CSP method is based on the simultaneous diagonalization of two real symmetric matrices proposed by Fukunaga [4]. The simultaneous diagonalization allows the

decomposition of raw EEG signals into two discriminated patterns extracted from two populations (classes) simultaneously maximizing the variance of one class and minimizing the variance of the other class. At the same time, a dimension reduction is achieved which is an important step for posterior classification.

This method has been successfully applied in BCI research for extraction and enhancement of ERD/ERS (Event Related (De)Synchronization) and Readiness Potential features associated with motor imagery paradigms [5], [6], [7]. Some variants of CSP were already proposed for the multiclass problem [8] [9]. A survey on CSP methods can be found in [10].

There are however very few applications of the CSP method on the detection of Event Related Potentials (ERP) such as the P300. As a relevant work, we point out the work in [11] where an extension of the CSP method is suggested, namely the Common Spatio-Temporal Patterns (CSTP). This approach incorporates time-delay embedding and non-centered covariance matrices into CSP to extract more prominent spatio-temporal patterns.

We propose here the application of standard CSP combined with a new approach of feature combination based on probabilistic models of spatial filtered data embedded in a Bayesian classifier. It is shown that CSP can be effectively used on P300. Also, we show that coherence can be used for channel selection enhancing pattern discrimination and simultaneously achieve a reduction of the required number of channels.

II. METHODS

A. Common Spatial Patterns

Within the P300 oddball principle context, we consider two spatio-temporal matrices \mathbf{X}_t and \mathbf{X}_{nt} with dimension $N \times T$, where N is the number of channels and T is the number of samples of the time series epoch of each channel. The matrix \mathbf{X}_t represents the P300 potential evoked by the target event and \mathbf{X}_{nt} represents the ongoing EEG for non-target events. The CSP method is based on the principal component decomposition of the the sum covariance \mathbf{R} of the target and non-target covariances

$$\mathbf{R} = \mathbf{R}_{nt} + \mathbf{R}_t \quad (1)$$

where \mathbf{R}_t and \mathbf{R}_{nt} are the normalized $N \times N$ spatial covariances computed from

$$\mathbf{R}_t = \frac{\mathbf{X}_t \mathbf{X}_t'}{\text{tr}(\mathbf{X}_t \mathbf{X}_t')} \quad \mathbf{R}_{nt} = \frac{\mathbf{X}_{nt} \mathbf{X}_{nt}'}{\text{tr}(\mathbf{X}_{nt} \mathbf{X}_{nt}')} \quad (2)$$

where $'$ represents the transpose operator and $\text{tr}(A)$ represents the trace of A .

The spatial filters are estimated from the overall set of trials gathered during training. Therefore it is used the average of the normalized covariances trials

$$\overline{\mathbf{R}}_t = \frac{1}{N_t} \sum_{i=1}^{N_t} \mathbf{R}_t(i) \quad \overline{\mathbf{R}}_{nt} = \frac{1}{N_{nt}} \sum_{i=1}^{N_{nt}} \mathbf{R}_{nt}(i) \quad (3)$$

where N_t and N_{nt} are the number of target and non-target trials in the training set. The averaged covariance matrix $\overline{\mathbf{R}}$ is factored through the application of the PCA as follows [12]

$$\overline{\mathbf{R}} = \overline{\mathbf{R}}_t + \overline{\mathbf{R}}_{nt} = \mathbf{A} \lambda \mathbf{A}' \quad (4)$$

where A is the orthogonal matrix of eigenvectors of $\overline{\mathbf{R}}$ and λ is the diagonal matrix of eigenvalues of $\overline{\mathbf{R}}$. A whitening transformation matrix \mathbf{W}

$$\mathbf{W} = \lambda^{-\frac{1}{2}} \mathbf{A}' \quad (5)$$

transforms the covariance matrix $\overline{\mathbf{R}}$ to I (identity matrix)

$$\mathbf{S} = \mathbf{W} \overline{\mathbf{R}} \mathbf{W}' = \mathbf{I}. \quad (6)$$

Applying the whitening transform to each individual class, we obtain

$$\mathbf{S}_t = \mathbf{W} \overline{\mathbf{R}}_t \mathbf{W}' \quad (7)$$

$$\mathbf{S}_{nt} = \mathbf{W} \overline{\mathbf{R}}_{nt} \mathbf{W}'. \quad (8)$$

From the above three equations it is straightforward that

$$\mathbf{S}_t + \mathbf{S}_{nt} = \mathbf{I} \quad (9)$$

Performing a PCA factorization to (7) and (8) then

$$\mathbf{S}_t = \mathbf{A}_t \lambda_t \mathbf{A}_t' \quad \mathbf{S}_{nt} = \mathbf{A}_{nt} \lambda_{nt} \mathbf{A}_{nt}' \quad (10)$$

From (9) and (10)

$$\mathbf{A}_t = \mathbf{A}_{nt} \quad (11)$$

and

$$\lambda_t = \mathbf{I} - \lambda_{nt}. \quad (12)$$

It means that both class patterns share the same eigenvectors and the respective eigenvalues are reversely ordered. The eigenvector with largest eigenvalue for one class has the smallest eigenvalue for the other class and vice versa. The first and last eigenvector are optimal eigenvectors to discriminate the two classes. Defining A_t and A_{nt} as the first and last eigenvectors with dimension $N \times 1$ the following spatial filters are designed

$$\mathbf{H}_t = \mathbf{A}_t' \mathbf{W} \quad (13)$$

$$\mathbf{H}_{nt} = \mathbf{A}_{nt}' \mathbf{W}. \quad (14)$$

The spatial filtered data is given by

$$\mathbf{Y} = \mathbf{H} \mathbf{X}. \quad (15)$$

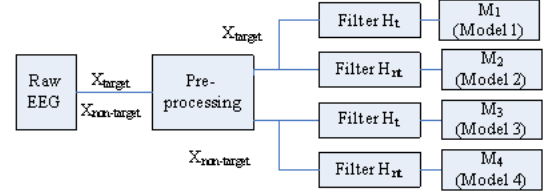


Fig. 1. Models obtained during training for projected data of target and non-target epochs.

B. Features and Classification

Usually, the features used for classification in motor imagery are the ratio between the variance of one filtered projection and the sum of the variances of all filtered projections. This method is suitable for motor imagery because the band power of μ and β rhythms are the main features. In the case of P300 pattern, the most important feature is the temporal structure and not the variance of the signal.

We present here a different method that relies on probabilistic models designed for each projected data and that therefore takes into account the temporal structure of P300 pattern. This procedure is described in Fig. 1. Four different models are obtained from the spatial filtering projection of target and non-target related potentials. For each projected sequence a conditional probability is computed, namely

$$p(\mathbf{x}_{ft}|M_1) \quad p(\mathbf{x}_{fnt}|M_2) \quad p(\mathbf{x}_{ft}|M_3) \quad p(\mathbf{x}_{fnt}|M_4) \quad (16)$$

where the vector \mathbf{x}_f represents the filtered projection. Let define w_t and w_{nt} respectively the class of target and non-target events. The posterior probability $p(w_i|\mathbf{X})$ ($i = t, nt$), i.e., the probability of a non spatially filtered data pattern $X_{N \times T}$ belong to class w_i is obtained through the Bayes rule [13]

$$p(w_t|\mathbf{X}) = \frac{P(w_t)p(\mathbf{x}_{ft}|M_1)p(\mathbf{x}_{fnt}|M_2)}{p(\mathbf{X})} \quad (17)$$

$$p(w_{nt}|\mathbf{X}) = \frac{P(w_{nt})p(\mathbf{x}_{ft}|M_3)p(\mathbf{x}_{fnt}|M_4)}{p(\mathbf{X})} \quad (18)$$

where $p(\mathbf{X})$ is the unconditional density of \mathbf{x} and $P(w_t), P(w_{nt})$ are the prior probabilities of each of the classes. The conditional probability $p(\mathbf{x}_f|M)$ is computed from the likelihood function under a gaussian distribution assumption

$$p(\mathbf{x}_f|\mu, \Sigma) = \frac{1}{(2\pi)^{n/2} |\Sigma|^{1/2}} \exp\left(-\frac{(\mathbf{x}_f - \mu)^T (\mathbf{x}_f - \mu)}{2\Sigma}\right) \quad (19)$$

where μ and Σ are the mean and covariance matrices computed for each class.

C. Coherence

Coherence gives a linear correlation between two signals as a function of the frequency. In the context of neurophysiology, it is used to measure the linear dependence and functional interaction between different brain regions. In this study,

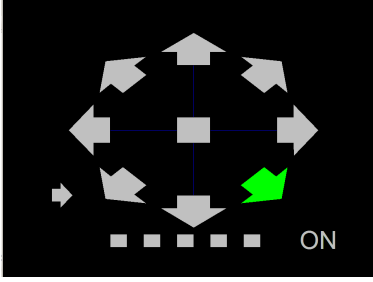


Fig. 2. P300 arrow paradigm. Each symbol is flashed during 100 ms and the time between flashes is 200 ms

coherence was used to select channels with strong inter-correlation. The goal is to reduce the number of channels for CSP filtering, and simultaneously improve or preserve the classification results obtained with a larger group of electrodes. Mathematically, the estimated coherence between signals x and y is computed by the magnitude squared coherence [14]

$$k_{xy}^2(f) = \frac{|\langle S_{xy}(f) \rangle|^2}{|\langle S_{xx}(f) \rangle| |\langle S_{yy}(f) \rangle|} \quad (20)$$

where $S_{xx}(f)$ and $S_{yy}(f)$ are respectively the power spectra of x and y , and S_{xy} is the cross-power spectrum. The spectra is estimated from the average ($\langle \cdot \rangle$) of the periodogram over the set of trials.

III. PARADIGM, DATA ACQUISITION AND CLASSIFICATION

A. Paradigm

The Paradigm is shown in Fig. 2 and was already presented in [15]. It is composed by 8 direction arrows, a stop square, a ON/OFF switch and 5 small squares with no special meaning. The paradigm was specifically designed to steer a robotic device, however the symbols can be used for other interpretations. Each symbol is randomly flashed with uniform distribution, therefore the event target occurs once on each 15 flashes providing an oddball paradigm.

B. Data Acquisition

Three healthy subjects participated at the experiments. The subjects were seated in front of a computer screen at about 60 cm. The EEG activity was recorded from 12 Ag/Cl electrodes at positions Fz, Cz, C3, C4, CPz, Pz, P3, P4, PO7, PO8, POz and Oz according to the internacional extended 10-20 standard system using a g.tec cap. The electrodes were referenced to the right mastoid and the ground was placed at AFz. The EEG channels were amplified with a gUSBamp (g.tec, Inc.) amplifier, bandpass filtered at 0.1-30 Hz and notch filtered at 50 Hz and sampled at 256 Hz. All electrodes were kept with impedances under $5K\Omega$.

Several sessions of 80 target epochs and 1120 non-target epochs were recorded. Each session takes about 4 minutes. These data sets were used for training and testing.

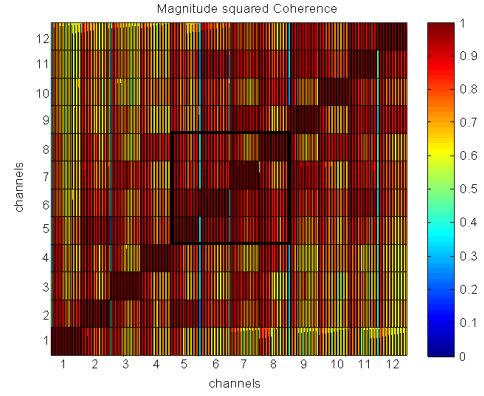


Fig. 3. Magnitude square coherence between channels. Channels are ordered from 1 to 12 according to Fz, Cz, C3, C4, CPz, Pz, P3, P4, PO7, PO8, POz and Oz. High level colors represent a high level of coherence.

C. Preprocessing and Classification

Each epoch has a duration of 1 second and is synchronized with the start of the event stimulus. The EEG signal is low-pass filtered by a 4th order Butterworth filter with 7 Hz cut frequency. Each epoch is normalized to zero mean and unit standard deviation.

After preprocessing of each individual channel it was applied an r-square measure (between target and nontarget epochs) for each instant time of the epoch-window using all collected epochs. This measure provides a level of discrimination between target and nontarget and therefore can be used to select the best time-window features (time segment within the 1 second epoch) and the best channels. The magnitude square coherence is computed to evaluate the degree of linear dependence between the 12 channels as shown in Fig. 3. From this color map it is possible to select a cluster of contiguous channels that evidence a strong inter-correlation (it was defined a threshold value of 0.9 for frequency in the range 0.5-7 Hz). The black square represents a possible cluster satisfying this threshold criteria, which corresponds to channels CPz, Pz, P3 and P4. Spatial filter CSP is then applied to this group of channels. Selecting the best time-window features, the conditional probabilities in (16) are computed through (19). The estimated class is reached using the Bayes decision function through the posterior probabilities (17) and (18) associated to each class.

IV. RESULTS

The top of Fig. 4 shows the average and standard deviation of the P300 pattern of the best channel (in this case P07) over 80 target epochs (blue) and 720 nontarget epochs (red). The overlapping of the two classes is a measure of how low is the discrimination between them. Also it is important to see that the standard deviation is almost constant over the time sequence. The bottom of Fig. 4 represents the average and standard deviation of CSP filtered data. The blue color represents the projected target epochs using filter H_t and red color the projected nontarget epochs through the filter H_{nt} . The plot shows clearly that the CSP filters separate the

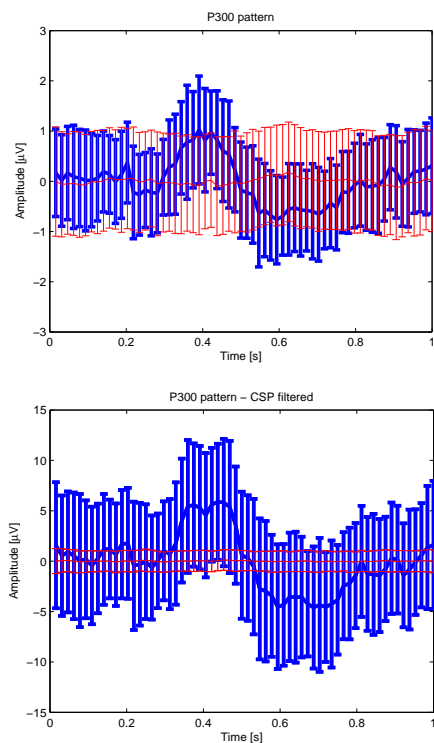


Fig. 4. Top: best channel mean and standard deviation over the set of target trial (blue) and nontarget trials (red); down: average and standard deviation of CSP filtered data from CPz, Pz, P3 and P4 channels.

two classes. Note however, that the current plot is the ideal situation where each epoch class is projected with filters that maximizes and minimizes the respective classes. In practice we will have to use the four models shown in Fig. 1 and not only two models.

Table I shows the achieved classification results with 3 subjects. Classification tests were performed using the best channel, the filtered CSP projections using all 12 channels and the filtered CSP projections using the channels selected through coherency. The use of CSP filter reduces the error rate when compared with single channel classification. In case of subject S2 the improvement of classification is not so significant. Actually, for this subject the individual channels showed a low target vs. nontarget discrimination. For subjects S1 and S3 the use of the selected channels demonstrates a better performance than the use of all channels which can confirm that CSP has a better performance when used with channels linearly correlated.

V. CONCLUSION

The presented work shows that CSP is a good spatial filter approach for the classification of P300 patterns. The probabilistic models of the spatial filtered data, embedded in the Bayesian classifier, represent reliable features. Also, it is proved that strong inter-channel correlation is an important factor that can enhance the discrimination provided with CSP filters. The achieved offline results are significant when compared with state of the art (e.g. see [1] and [11]).

TABLE I
ERROR RATE CLASSIFICATION (%)

trials	method	Subjects		
		S1	S2	S3
1	best ch	18.3	18.4	11.22
	CSP all ch	15.0	14.2	10.1
	CSP sel. ch	15.0	18.5	8.3
2	best ch	12.5	10.6	6.5
	CSP all ch	10.2	8.0	3.0
	CSP sel. ch	10.0	12.8	2.8
5	best ch	3.0	6.0	2.7
	CSP all ch	1.9	5.4	1.0
	CSP sel. ch	1.2	5.4	0.5

ACKNOWLEDGMENT

This work has been in part supported by Fundação para a Ciência e Tecnologia (FCT), under Grant PTDC/EEA-ACR/72226/2006. Gabriel Pires would like also to thank the support of FCT through the research fellowship SFRH/BD/29610/2006.

REFERENCES

- [1] L. Farwell and E. Donchin, "Talking off the top of your head: toward a mental prosthesis utilizing event related brain potentials," *Electr. and Clinical Neuroph.*, vol. 70, no. 6, pp. 510–523, 1988.
- [2] D. J. McFarland, L. McCane, S. V. David, and J. R. Wolpaw, "Spatial filter selection for eeg-based communication," *Journal of Electroencephalography and clinical Neurophys.*, vol. 103, pp. 386–394, 1997.
- [3] A. Soong and Z. Koles, "Principal-component localization of the sources of the background eeg," *IEEE Transactions on Biomedical Engineering*, vol. 42, no. 1, pp. 59–67, Jan. 1995.
- [4] K. Fukunaga, *Introduction to Statistical Pattern Recognition, Second Edition*. Morgan Kaufmann - Academic Press, 1990.
- [5] H. Ramoser, J. Muller-Gerking, and G. Pfurtscheller, "Optimal spatial filtering of single trial eeg during imagined hand movement," *IEEE Trans. on Rehabilitation Engineering*, vol. 8, no. 4, pp. 441–446, Dec 2000.
- [6] J. Miller-Gerking, G. Pfurtscheller, and H. Flyvbjerg, "Designing optimal spatial filters for single-trial eeg classification in a movement task," *Journal of Clinical Neurophysiology*, vol. 110, no. 5, pp. 787–798, 1999.
- [7] Y. Li, X. Gao, H. Liu, and S. Gao, "Classification of single-trial electroencephalogram during finger movement," *IEEE Transactions on Biomedical Engineering*, vol. 51, no. 6, pp. 1019–1025, June 2004.
- [8] G. Dornhege, B. Blankertz, G. Curio, and K.-R. Muller, "Boosting bit rates in noninvasive eeg single-trial classifications by feature combination and multiclass paradigms," *Biomedical Engineering, IEEE Transactions on*, vol. 51, no. 6, pp. 993–1002, June 2004.
- [9] Y. Wang, P. Berg, and M. Scherg, "Common spatial subspace decomposition applied to analysis of brain responses under multiple task conditions: a simulation study," *Clinical Neurophysiology*, vol. 110, pp. 604–614, 1999.
- [10] B. Blankertz, R. Tomioka, S. Lemm, M. Kawanabe, and K.-R. Muller, "Optimizing spatial filters for robust eeg single-trial analysis," *Signal Processing Magazine, IEEE*, vol. 25, no. 1, pp. 41–56, 2008.
- [11] D. J. Krusienski, W. Sellers, and T. M. Vaughan, "Common spatio-temporal patterns for the p300 speller," *3rd IEEE EMBS Intern. Conf. on Neural Engineering*, pp. 421–424, May 2007.
- [12] I. T. Jolliffe, *Principal Component Analysis, Second Edition*. Springer Series in Statistics, 2002.
- [13] F. Heijden, R. Duin, D. Ridder, and D. Tax, *Classification, Parameter Estimation and State Estimation*. John Wiley & Sons, 2004.
- [14] J. S. Bendat and A. G. Piersol, *Random data - Analysis and Measurement Procedure*. John Wiley & Sons, Inc, 2000.
- [15] G. Pires, M. Castelo-Branco, and U. Nunes, "Visual p300-based bci to steer a wheelchair: A bayesian approach," *30th Annual Int. Conf. of the IEEE Eng. in Medicine and Biology Society, EMBS2008*, pp. 658–661, Aug. 2008.